Journal of Biomechanics 70 (2018) 59–66

Contents lists available at ScienceDirect

Journal of Biomechanics

journal homepage: www.elsevier.com/locate/jbiomech
www.JBiomech.com

The equivalence of multi-axis spine systems: Recommended stiffness limits using a standardized testing protocol

Timothy P. Holsgrove [a,b,*], Dhara B. Amin [c], Sonia Ramos Pascual [b], Boyin Ding [d], William C. Welch [e], Sabina Gheduzzi [b], Anthony W. Miles [b], Beth A. Winkelstein [e,f], John J. Costi [c]

[a] Department of Engineering, College of Engineering, Mathematics & Physical Sciences, University of Exeter, Exeter, UK
[b] Centre for Orthopaedic Biomechanics, Department of Mechanical Engineering, University of Bath, Bath, UK
[c] Biomechanics & Implants Research Group, The Medical Device Research Institute, Flinders University, Adelaide, SA, Australia
[d] School of Mechanical Engineering, The University of Adelaide, Adelaide, SA, Australia
[e] Department of Neurosurgery, University of Pennsylvania, PA, USA
[f] Department of Bioengineering, School of Engineering and Applied Science, University of Pennsylvania, PA, USA

ARTICLE INFO

Article history:
Accepted 6 September 2017

Keywords:
Multi-axis
Six-axis
Spine testing
Spine simulator
Test machines
Test systems

ABSTRACT

The complexity of multi-axis spine testing often makes it challenging to compare results from different studies. The aim of this work was to develop and implement a standardized testing protocol across three six-axis spine systems, compare them, and provide stiffness and phase angle limits against which other test systems can be compared. Standardized synthetic lumbar specimens (n = 5), comprising three springs embedded in polymer at each end, were tested on each system using pure moments in flexion–extension, lateral bending, and axial rotation. Tests were performed using sine and triangle waves with an amplitude of 8 Nm, a frequency of 0.1 Hz, and with axial preloads of 0 and 500 N. The stiffness, phase angle, and R^2 value of the moment against rotation in the principal axis were calculated at the center of each specimen. The tracking error was adopted as a measure of each test system to minimize non-principal loads, defined as the root mean squared difference between actual and target loads. All three test systems demonstrated similar stiffnesses, with small (<14%) but significant differences in 4 of 12 tests. More variability was observed in the phase angle between the principal axis moment and rotation, with significant differences in 10 of 12 tests. Stiffness and phase angle limits were calculated based on the 95% confidence intervals from all three systems. These recommendations can be used with the standard specimen and testing protocol by other research institutions to ensure equivalence of different spine systems, increasing the ability to compare in vitro spine studies.

1. Introduction

Replicating in vivo loads in the spine is a critical aspect of in vitro spine testing; however, the complexity of the mechanical properties of the intervertebral disc, facet joints, and the numerous muscles and ligaments that actuate and guide motion at each vertebral level make doing so a considerable challenge (Holsgrove et al., 2015b; Jaumard et al., 2011).

There are many six-axis testing systems that have been used for the biomechanical testing of the spine (Chung et al., 2002; Ding et al., 2014; Holsgrove et al., 2014; Ilharreborde et al., 2010; Kelly and Bennett, 2013; Martínez et al., 2013; Stokes et al., 2002; Wilke et al., 1994; Wilke et al., 2016), however, the designs and control capabilities of those testing systems vary considerably. Additionally, despite previous studies having demonstrated the large changes in the mechanical properties of spinal specimens due to a preload (Gardner-Morse and Stokes, 2003; Holsgrove et al., 2015a; Panjabi et al., 2001; Tawackoli et al., 2004) and the method of preload application (Cripton et al., 2000), testing rate (Costi et al., 2008; Gay et al., 2008), and testing environment (Costi et al., 2002; Pflaster et al., 1997; Wilke et al., 1998a), the standardization of in vitro methods is still lacking, despite previous recommendations (Goel et al., 2006; Wilke et al., 1998b), which often makes it difficult, if not impossible, to compare different biomechanical studies (Holsgrove et al., 2015b).

Whilst a multi-center study has demonstrated that consistent results can be acquired in the pure moment testing of cadaveric specimens without a physiological preload (Wheeler et al., 2011),

* Corresponding author at: Unit L, Innovation Building, Streatham Campus, University of Exeter, Exeter EX4 4QF, UK.
E-mail address: t.holsgrove@exeter.ac.uk (T.P. Holsgrove).

http://dx.doi.org/10.1016/j.jbiomech.2017.09.010
0021-9290/

there is limited data to compare multi-axis test systems with axial preloads applied to specimens, and there is no data in regard to a standard test method with which to compare different test systems. Therefore, the aim of this study was to use existing standards (British Standards Institution, 2009, 2012), and spine testing recommendations (Goel et al., 2006; Holsgrove et al., 2015b; Wilke et al., 1998b), to develop a standard multi-axis test protocol to compare different systems, using synthetic lumbar spinal motion segments. The protocol was then implemented on three systems, and the stiffness and phase angle data were used to establish acceptable stiffness and phase angle limits.

2. Materials and methods

Three multi-axis testing systems were used. One custom assembly (GT1) was capable of position or load control in six degrees of freedom (6DOF) using a gimbal head mounted on translational axes, with a load capacity of ±500 N in shear loading, ±4000 N in axial compression-tension, and ±35 Nm in all rotational axes (Holsgrove et al., 2017) (Fig. 1a). Another custom system (HEX) adopted a hexapod design based on the concept of the Stewart Platform, with six actuators linking the base and test platforms, which was also capable of position and load control in 6DOF (Lawless et al., 2014), with a load capacity of ±7.2 kN in shear, 18 kN in axial compression-extension, and 1.4 kNm in all rotational axes (Fig. 1b). The final system (GT2) was a commercially available dual axis MTS servo-hydraulic testing machine (370.02 FlexTest 60; MTS Systems Corp., Eden Prairie, MN, USA) combined with an MTS kinematic spine system (Bionix Spine Kinematics System; MTS Systems Corp.) to provide position or load control in four axes (axial compression-tension, flexion-extension, lateral bending, and axial rotation), with a custom dual platform of linear guide rails providing passive axes in anteroposterior and mediolateral translation (Fig. 1c). GT2 had a load capacity of 580 N in shear, 1160 N in axial compression-extension, and 20 Nm in all rotational axes. However, the load cell used for the control of the axial preload had a capacity of 22 kN. All three systems measured position directly from sensors mounted on the system load frames.

After completing all tests at on each system, the tests were repeated on the original system (GT1) to ensure that no damage had occurred to the specimens.

2.1. Synthetic specimen design

Six synthetic lumbar specimens were fabricated, allowing standardized comparisons to be made between different multi-axis systems. The synthetic specimen design (Fig. 2) was based on the only international standard for pre-clinical spine testing that describes spring-based anterior supports for the lumbar region of the spine, *ISO 12189:2008* (British Standards Institution, 2009); the dimensions and mechanical properties of the springs used for the anterior support are outlined in *ISO 10243:2010+A1:2011* (British Standards Institution, 2012).

The criterion of *ISO 12189:2008* is limited to compression testing, where three heavy-duty die cast springs of Ø25 mm and 25 mm length are placed in circular recesses within each test block. However, in order to apply pure moments to the specimens, it was necessary to rigidly fix the springs at each end. This was accomplished by using springs with a length of 76 mm, and embedding each end in a two-part fast-curing liquid polymer (Smooth Cast® 300; Smooth-On, Inc.; Macungie, PA) using a potting jig (Fig. 2c) to ensure that the spacing and resulting free-length was 25 mm. Each spring had a stiffness of approximately 99 N/mm but once embedded with a free-length of 25 mm, the stiffness was expected to be approximately 375 N/mm (British Standards Institution, 2012), giving an overall specimen compressive stiffness of approximately 1125 N/mm.

The same six polymer/spring specimens were used for testing on all three systems. Additionally, the cylindrical part of the specimen pots, to which the specimens were fixed using radial screws, were used for testing of the specimens to ensure consistent fixation to each test system (Fig. 2d).

2.2. Test regime

Twelve tests (three loading directions × two waveforms × two preloads) were completed on each system. Pure moments of ±8 Nm were individually applied in flexion-extension, lateral bending, and axial rotation (ASTM International, 2011; Kelly and Bennett, 2013; Lawless et al., 2014) to the specimens on each system according to a standardized protocol (Table 1). All axes were tested first without a preload, and then with a 500 N axial preload (Costi et al., 2008; Cripton et al., 2000; Holsgrove et al., 2015a),

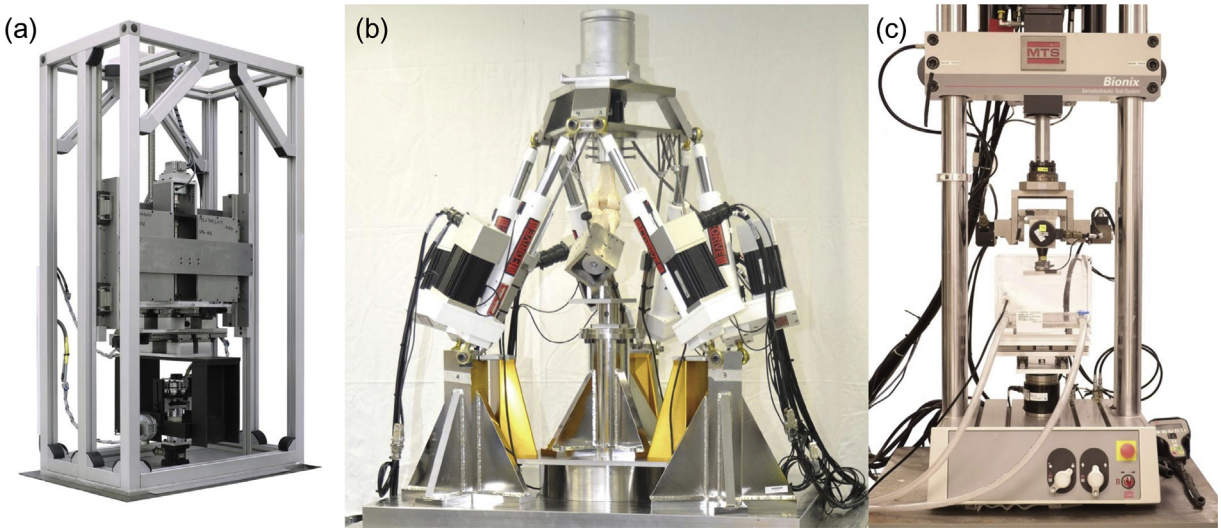

Fig. 1. The three multi-axis test systems of the present study. A custom system (GT1) comprising a gimbal and translation platform capable of 6DOF position or load control (a). A custom hexapod system (HEX) with six actuators linking the base and test platforms to provide 6DOF position or load control (b). A commercial servo-hydraulic test system (GT2) capable of position or load control in four axes, with a custom passive platform to minimize anteroposterior and mediolateral shear loads (c).

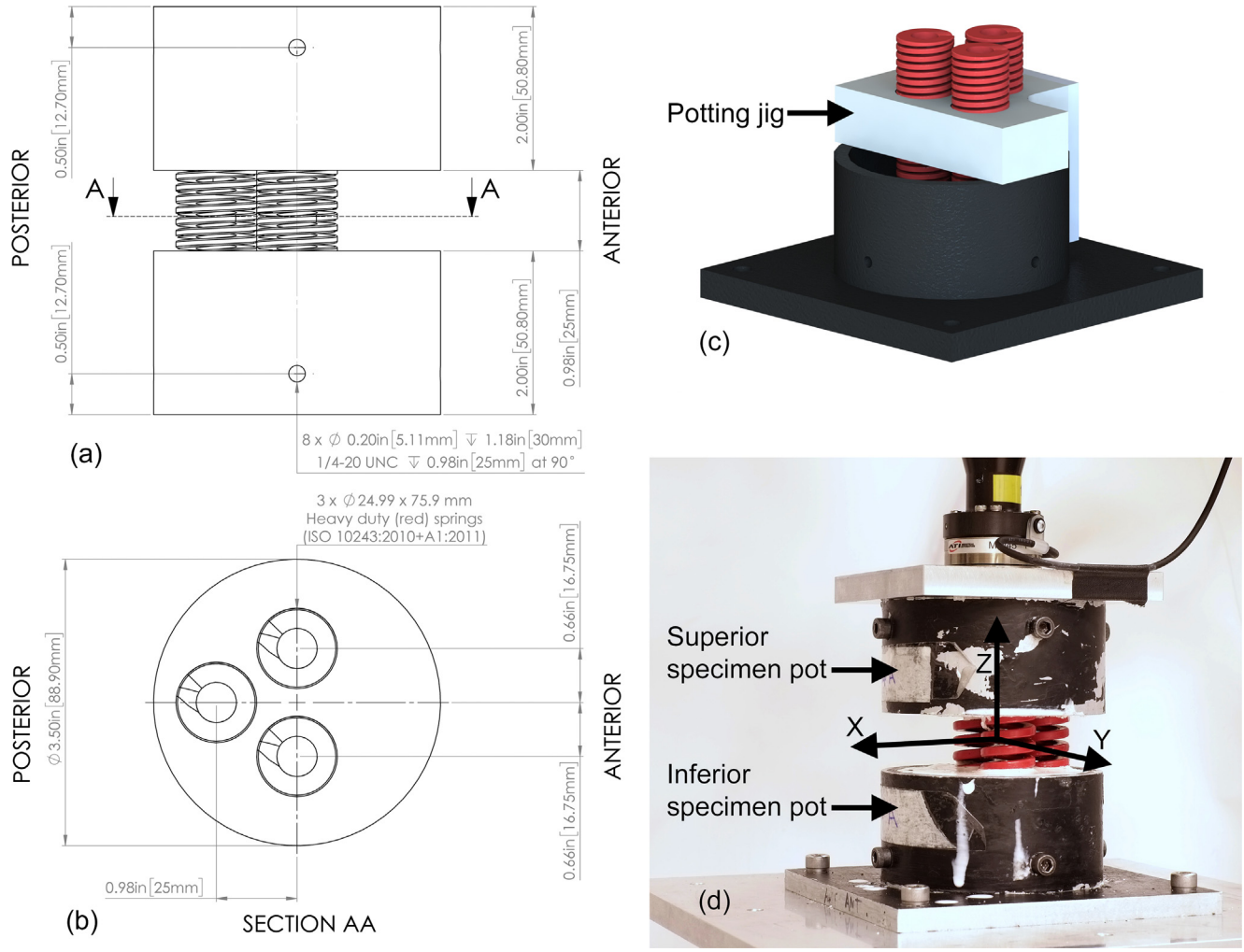

Fig. 2. Spring spacing of the synthetic lumbar specimens based on ISO 12189:2008 in the lateral view (a), and an axial cross-section AA (b). Schematic of the springs arranged for standardized potting in fast-curing polymer using a jig (c). A potted specimen mounted on a test system with the coordinate system denoted (d).

which was applied as a vertical vector. Pure moments were applied using both sine and triangle waveforms for each test condition at 0.1 Hz. The time, load and position data were acquired at 100 Hz for all tests. Five cycles were applied for each test, with the first two cycles used for preconditioning, and the last three used for data analysis (Holsgrove et al., 2015a; Holsgrove et al., 2017; Wilke et al., 1998b).

The coordinate system used was based on previous recommendations for spinal testing (Holsgrove et al., 2015b; Wilke et al., 1998b), with the x, y, and z axes corresponding to anterior shear, left lateral shear, and axial tension respectively (Fig. 2d). Prior to testing, the specimen pots were mounted on the test machine, and the loads were offset to zero. The specimen was then fixed into the test system with the geometric center aligned along the z axis. The datum of x and y axes was also adjusted to be at the geometrical center of the specimen in the GT1 and HEX; the axial position of the x and y axes was not adjustable on GT2.

Once positioned, the test system was set to load control with a zero set point in all six axes; in the case of GT2, the four active axes were operated in load control with a zero set point, and the passive axes in the anteroposterior and mediolateral directions were allowed to move freely to maintain minimal shear loading. The zero load condition was maintained for five minutes prior to commencing pure moment tests, which were completed in the order of flexion-extension, lateral bending, and axial rotation, with sine waves completed in all axes prior to the completion of triangle waves. Each test of five cycles took 50 s to complete, and a one minute recovery period was employed between each test. The axial preload of 500 N was then applied and equilibrated with all other axes maintained in the zero load condition for five minutes prior to repeating the pure moment tests using sine and triangle waves. The order of testing specimens was randomized at each institution.

2.3. Data analysis

The load data were adjusted to the geometrical center of the specimen using rigid body transformations. Transformation matrices were calculated based on position and angle of the load cell datum relative to the specimen center on each system during each test. These allowed the required translations and rotations of the load matrix to be completed, and the transformed load data were then used to calculate the stiffness, phase angle, R^2 value and tracking errors for each test. The stiffness in the test axis was calculated over the entire load-unload period of the last three cycles. Stiffness was calculated from the principal axis moment and rotation data using the linear least squares method, and the R^2 value was calculated to assess the linearity. The phase angle for the principal axis of each test was calculated between the input moment and measured rotation for the last three cycles using the cross spectral density estimate function (Matlab: CSD.m) to assess lag

Table 1
The standardized pure moment testing protocol.

Step	Description
1	Mount specimen pots into the test system
2	Offset all loads to zero
3	Rigidly fix the specimen into the specimen pots
4	Adjust the position to minimize the loads in all axes
5	Offset all positions to zero
6	Change all active axes to load control with a zero set point
7	Five-minute equilibration period
8	Five, 0.1 Hz sine wave cycles of ±8 Nm in flexion-extension
9	One-minute recovery period
10	Five, 0.1 Hz sine waves of ±8 Nm in lateral bending
11	One-minute recovery period
12	Five, 0.1 Hz sine waves of ±8 Nm in axial rotation
13	One-minute recovery period
14	Five, 0.1 Hz triangle waves of ±8 Nm in flexion-extension
15	One-minute recovery period
16	Five, 0.1 Hz triangle waves of ±8 Nm in lateral bending
17	One-minute recovery period
18	Five, 0.1 Hz triangle waves of ±8 Nm in axial rotation
19	Change the axial load set point to 500 N of compression
20	Five-minute equilibration period
21	Repeat steps 8–18
22	Return axial load set point to 0 N
23	Change all active axes to position control
24	Remove the specimen
25	Repeat steps 3–24 for all other specimens

due to deformation of the potting material and system compliance (Amin et al., 2015; Costi et al., 2008). Additionally, the ability of each system to minimize non-primary loads was assessed by calculating the tracking error of the non-principal axes for each test using the mean root mean squared (RMS) difference between the target and the actual load at the geometric center of the specimen. The target loads were 0 N and 0 Nm except for the target axial load of 500 N compression during tests with a preload. The tracking error of the five non-principal axes in each test were grouped into non-principal moments, shear forces, and axial force, in order to provide an overall summary of the capability of each system to minimize loads. It should be noted that the HEX control system completed rigid body transformations of the load data in real-time. This was not possible with the GT1 and GT2 systems, so the rigid body transformations were completed in post-processing, and the transformed data used for the system comparisons.

To ensure that the specimens had not been damaged during the tests, the stiffness and phase angle of the three systems and the repeat testing on the original system were compared using repeated measures ANOVAs, and in cases of significance a paired *t*-test post hoc analysis with Bonferroni correction was used (IBM SPSS Statistics 23.0.0.0; IBM Corporation; Armonk, NY). The stiffness, phase angle, and tracking error measurements of the three systems were then compared without the repeat tests using the same statistical method, and this data used to compare the systems and develop the testing recommendations. All statistical analyses were completed with a significance level of 0.05.

3. Results

The tests on each system demonstrated that the use of standardized synthetic specimens led to a low variation in stiffness between specimens on each test system (interquartile range (IQR) within 14% of the median), though one specimen was substantially lower in stiffness than other specimens. That specimen had a stiffness of more than 3 times the IQR less than the median in 26 of the 36 tests completed (12 tests at three institutions); therefore, the specimen was regarded as an outlier and was not included in the data analysis. This exclusion reduced the maximum IQR across all tests to 12.4%.

There were no differences in the phase angle between the original tests on GT1 and the repeated tests completed after testing on all three systems. There was a significant difference in the stiffness of one repeated test ($p = 0.004$ for flexion-extension, with a 500 N preload, and a triangle wave), though the magnitude of change was extremely small, with a maximum change in specimen stiffness of only 0.05 Nm/°. The stiffness across test systems showed good agreement (Fig. 3), with no significant differences between any systems without a preload, or in axial rotation with a preload. There were small but significant differences in flexion-extension with a preload between systems GT1 and GT2 ($p = 0.002$ for sine waves; 0.003 for triangle waves). There were also small but significant differences between all systems in lateral bending with a preload: systems GT1 and GT2 ($p = 0.002$ for sine waves; 0.003 for triangle waves); systems GT1 and HEX ($p = 0.001$ for sine waves; 0.002 for triangle waves); and systems GT2 and HEX ($p = 0.004$ for sine waves; 0.012 for triangle waves). However, whilst significant differences were detected, the maximum percentage difference between systems was 13.14%, and the mean (standard deviation (SD)) difference was only 5.80(3.90)%. The R^2 values of the stiffness plots demonstrated that the stiffness was highly linear (Fig. 4), with mean (SD) R^2 values across all tests of 0.996(0.004) on GT1, 0.997(0.002) on GT2, and 0.995(0.002) on HEX.

The phase angle between the principal test axis moment and rotation (Fig. 5) varied more across systems than the stiffness, and also demonstrated differences in phase magnitude between axes of the same system (Fig. 5). GT1 had relatively low phase across all tests, and GT2 had an extremely low phase angle in lateral bending tests. The phase was significantly different between all test systems in all lateral bending tests ($p < 0.013$). In all flexion-extension tests, the phase of GT1 was significantly lower than GT2 ($p < 0.012$) and HEX ($p < 0.010$), but there were no differences between GT2 and HEX. In axial rotation tests with a 500 N preload, the phase of GT1 was significantly lower than GT2 using sine waves ($p < 0.001$), and significantly lower than GT2 and HEX using triangle waves ($p < 0.036$).

There were significant differences in the tracking error between at least two systems in 32 of 36 comparisons (Table 2), despite all systems generally maintaining loads close to target set points. However, the axial tracking error was relatively high in all tests with GT2, but this was particularly true in flexion-extension tests. The axial force tracking error in HEX was also relatively high without a preload, and substantially higher than respective tests with an axial preload (Table 2).

4. Discussion

The aim of this study was to develop and implement a standardized testing protocol to compare multi-axis test systems. The synthetic lumbar spinal specimens were modified from the compression only configuration of the anterior support design of ISO 12189:2008 (British Standards Institution, 2009) by embedding the springs in a polymer, thus allowing a pure moment protocol to be completed. Since this design was relatively simple to fabricate, it can be easily adopted to assess whether other test systems are in line with the results of the present study. One specimen was identified as an outlier, which may have been caused by improper potting of the springs within the polymer. This outlier specimen was identified as the stiffness was more than three times the IQR less than the median stiffness in the majority of tests across all three systems. It is recommended that other institutions using similar specimens identify outliers using the same method.

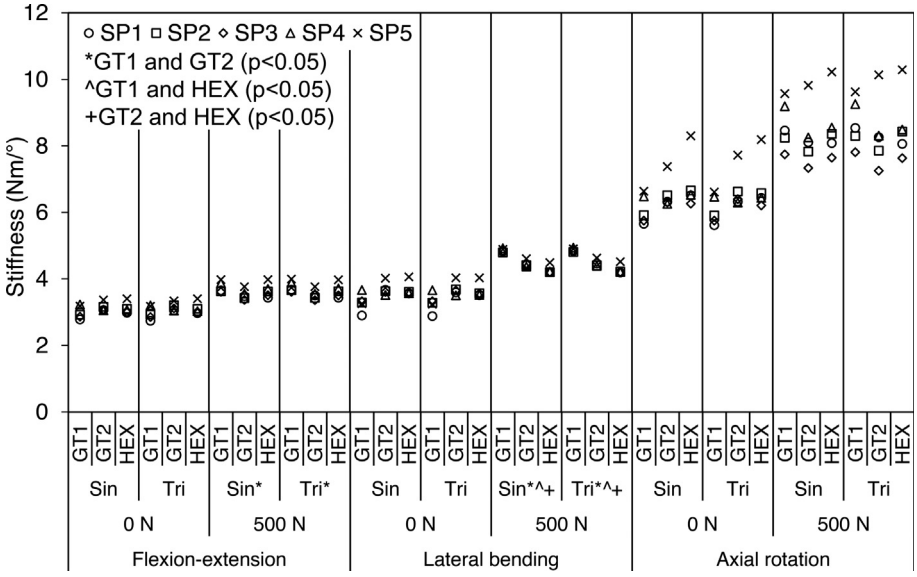

Fig. 3. Stiffness of each specimen (n = 5) in flexion-extension, lateral bending, and axial rotation tests with a 0 N and 500 N preload using sine and triangle waveforms on three different test systems (GT1, GT2, and HEX). Statistical significance ($p < 0.05$) is denoted for comparisons between each system for each test condition: *GT1 and GT2; ^GT1 and HEX; +GT2 and HEX.

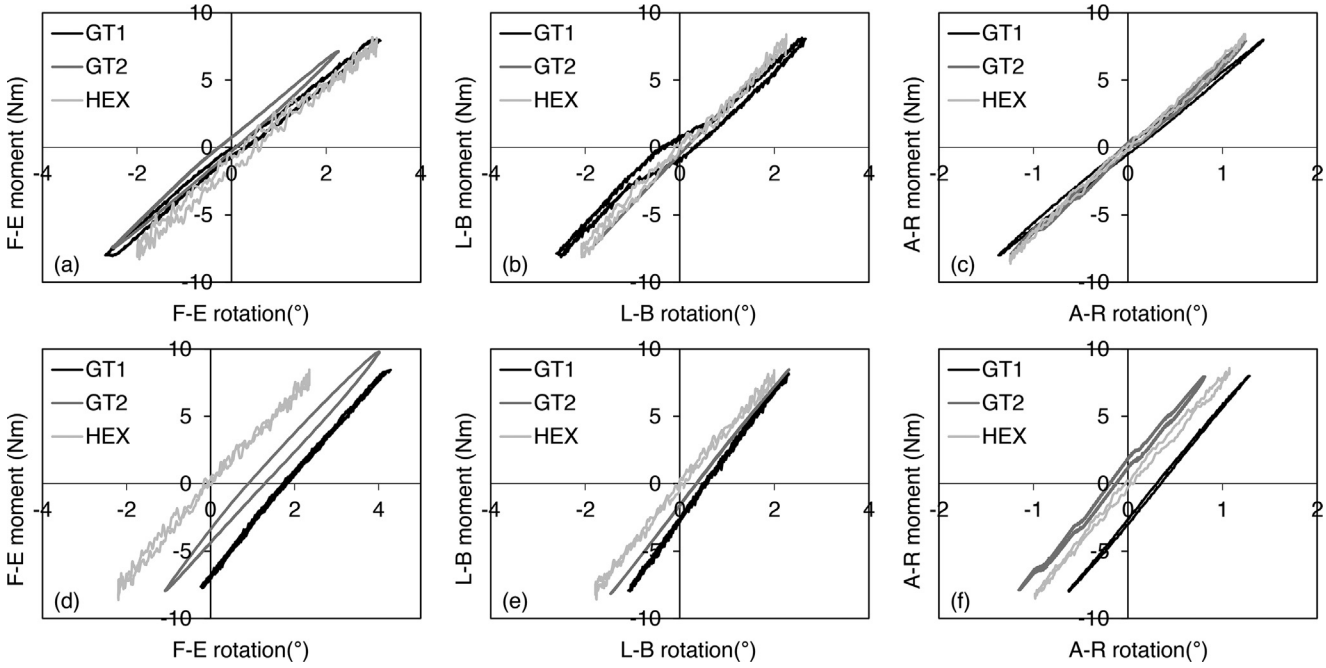

Fig. 4. Moment against rotation plots of a single specimen using a sine wave profile on each test system (GT1, GT2, and HEX) measured at the geometric center of the specimen with an axial preload of 0 N in flexion-extension (a), lateral bending (b), and axial rotation (c), and with an axial preload of 500 N in flexion-extension (d), lateral bending (e), and axial rotation (f).

The mean stiffness measured on the GT1 system was lower compared to GT2 and HEX without a preload, but higher with the axial preload of 500 N. This suggests that there was some system compliance without the axial load, which would also account for the increased hysteresis visible in lateral bending without a preload (Fig. 4b), compared to the test with a 500 N preload (Fig. 4e). The GT1 system comprises zero-backlash gears and couplings, but it is possible that there was some compliance in the gear assemblies or fixtures, which was eliminated through the application of the axial preload.

The relatively high axial load tracking error of GT2, and of HEX without a preload (Table 2) may be due to the respective load cell capacities of 22.0 kN and 18.0 kN used to control the axial load compared to that of 4.4 kN in GT1. This demonstrates that working close to the load cell capacity provides a control system advantage, though it is likely that some of the tracking error in HEX was also due to the backlash of the ball-screw actuators (Ding et al., 2015). The moving mass of HEX is also higher than the GT1 or GT2 systems, which increases the difficulty to maintain low tracking error in dynamic loading conditions, and may account for the increased

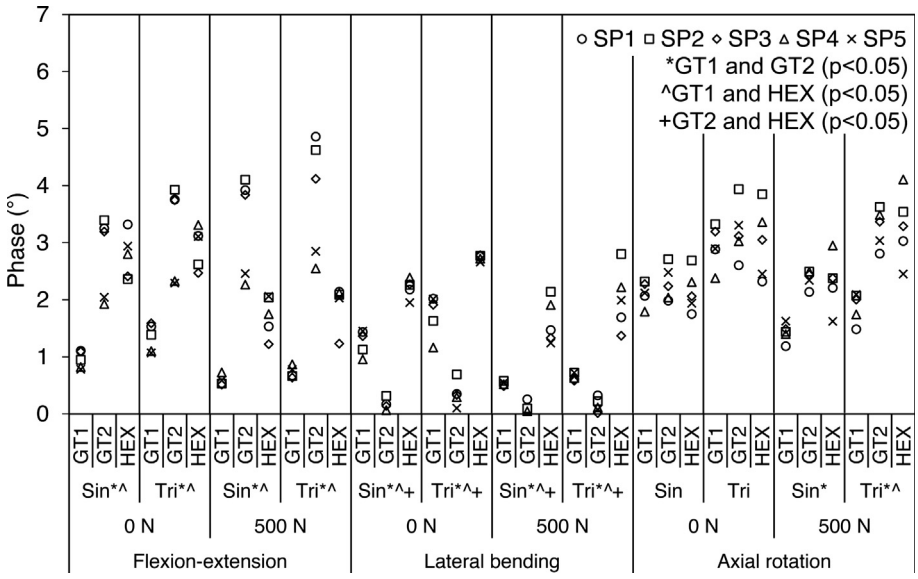

Fig. 5. Phase between the principal test axis rotation and moment for each specimen (n = 5) in flexion-extension, lateral bending, and axial rotation tests with a 0 and 500 N preload using sine and triangle waveforms on three different test systems (GT1, GT2, and HEX). Statistical significance ($p < 0.05$) is denoted for comparisons between each system for each test condition: *GT1 and GT2; ^GT1 and HEX;+GT2 and HEX.

Table 2
The mean (SD) RMS tracking error of non-principal moments, shear forces, and axial force for each system in flexion-extension, lateral bending, and axial rotation. Statistical significance ($p < 0.05$) is denoted for comparisons between each system for each test condition: *GT1 and GT2; ^GT1 and HEX; +GT2 and HEX.

	Non-principal moments (Nm)											
	Flexion-extension				Lateral bending				Axial rotation			
	0 N		500 N		0 N		500 N		0 N		500 N	
System	Sin*^+	Tri*^	Sin^	Tri	Sin*^+	Tri*^+	Sin*^+	Tri	Sin*^	Tri*^+	Sin*^	Tri
GT1	0.10(0.01)	0.09(0.01)	0.12(0.02)	0.13(0.02)	0.08(0.00)	0.07(0.00)	0.19(0.01)	0.19(0.01)	0.09(0.01)	0.09(0.01)	0.25(0.00)	0.25(0.00)
GT2	0.19(0.06)	0.22(0.02)	0.21(0.09)	0.19(0.08)	0.19(0.04)	0.20(0.04)	0.41(0.09)	0.40(0.14)	0.40(0.09)	0.48(0.04)	0.57(0.19)	0.61(0.28)
HEX	0.29(0.02)	0.27(0.03)	0.27(0.02)	0.25(0.03)	0.31(0.04)	0.29(0.02)	0.32(0.04)	0.32(0.03)	0.29(0.01)	0.28(0.01)	0.36(0.03)	0.35(0.03)
	Shear forces (N)											
	Flexion-extension				Lateral bending				Axial rotation			
	0 N		500 N		0 N		500 N		0 N		500 N	
System	Sin*^	Tri*^+	Sin*^	Tri*^+	Sin*^+	Tri*^+	Sin*^+	Tri*^+	Sin*^+	Tri*^+	Sin*^+	Tri*^+
GT1	0.58(0.04)	0.58(0.04)	0.63(0.03)	0.65(0.03)	0.62(0.06)	0.61(0.05)	0.60(0.04)	0.61(0.03)	0.55(0.04)	0.54(0.01)	0.58(0.04)	0.57(0.03)
GT2	5.92(0.79)	6.47(0.24)	6.09(1.02)	6.19(0.88)	6.36(0.48)	6.75(0.45)	6.33(0.22)	6.45(0.71)	5.31(1.19)	6.24(0.52)	3.82(0.88)	4.24(0.57)
HEX	7.65(1.82)	7.48(1.46)	7.92(0.69)	8.20(1.03)	8.22(1.87)	8.26(1.59)	10.9(1.75)	10.4(2.37)	8.49(0.86)	8.88(0.75)	9.67(1.53)	9.77(2.38)
	Axial force (N)											
	Flexion-extension				Lateral bending				Axial rotation			
	0 N		500 N		0 N		500 N		0 N		500 N	
System	Sin*^	Tri*^	Sin*+	Tri*+	Sin^	Tri*^	Sin*+	Tri*^+	Sin*^	Tri*^	Sin*^+	Tri
GT1	1.93(0.07)	1.86(0.08)	1.68(0.05)	1.70(0.08)	1.60(0.08)	1.47(0.04)	1.27(0.04)	1.31(0.03)	1.38(0.10)	1.33(0.08)	1.36(0.04)	1.37(0.03)
GT2	36.4(12.7)	39.5(15.7)	51.0(11.9)	51.6(19.9)	16.1(11.8)	22.2(13.6)	37.4(24.9)	36.6(22.0)	22.1(13.9)	44.8(27.2)	28.6(11.6)	28.2(26.9)
HEX	57.4(4.78)	49.4(3.81)	2.30(0.36)	2.27(0.32)	24.4(12.4)	21.5(10.8)	1.14(0.29)	0.98(0.53)	27.6(3.18)	25.0(2.75)	0.30(0.17)	0.27(0.09)

magnitude and variation in the phase angle with this system (Fig. 5). However, it should be noted that the phase angle results across all systems was low, with mean (SD) phase angles across all tests of 1.34(0.73)°, 2.08(1.50)°, and 2.39(0.65)° for GT1, GT2, and HEX respectively; this is result of the test specimen exhibiting elastic behavior, without the viscoelasticity or damping that would be present in a biological spine specimen. The tracking error of HEX was also higher than GT1 and GT2 in many comparisons (Table 3), and this is likely due to the system complexity, which requires that all six actuators move in order to apply movement in a single anatomical plane. However, this complexity also provides greater flexibility in applying complex loads. The tuning of such systems is also a critical factor in maintaining desired loads at physiological loading rates, though a variety of methods were employed in the present study: manual tuning (GT1); auto-tuning (GT2); and adaptive tuning (HEX) (Lawless et al., 2014).

The ability to adjust the coordinate system relating to the application of loading with both GT1 and HEX meant that the initial center of rotation could be positioned at the geometric center of the specimen. This, combined with the orientation of the load cell of GT1 being the same as the specimen center, enabled the shear loads to be maintained close to the zero set point in all tests on this system (Table 2). Such adjustments were not possible with GT2, leading to relatively large translations of the XY platform during

Table 3
Recommended stiffness and phase limits based on the 95% confidence intervals of tests across all three systems of the present study.

Parameter	0 N preload					
	FE		LB		AR	
	Sin	Tri	Sin	Tri	Sin	Tri
Stiffness upper limit (Nm/°)	3.26	3.26	3.87	3.87	7.57	7.47
Stiffness lower limit (Nm/°)	2.82	2.80	3.05	3.03	5.70	5.68
Phase upper limit (°)	3.39	3.93	2.35	2.78	2.56	3.63
Phase lower limit (°)	0.82	1.12	0.02	0.17	1.83	2.45
	500 N axial preload					
Stiffness upper limit (Nm/°)	3.90	3.91	4.90	4.91	9.43	9.47
Stiffness lower limit (Nm/°)	3.38	3.39	4.15	4.14	7.45	7.41
Phase upper limit (°)	4.09	4.72	1.96	2.49	2.73	3.82
Phase lower limit (°)	0.50	0.64	0.00	0.04	1.29	1.65

flexion-extension, and lateral bending tests. It is likely that this altered the load transfer through the specimen, which may have contributed to the relatively high axial force tracking errors in flexion-extension and lateral bending with the 500 N preload compared to the same tests without a preload (Table 2).

The stiffness and phase results were consistent between the sine and triangle waveforms, suggesting that it may not be necessary to use both waveforms in future tests that adopt the standardized protocol. Sine waveforms are commonly used in spine testing to simplify test control, and approximate physiologic motion (Amin et al., 2015; Chamoli et al., 2015; Costi et al., 2008; Wilke et al., 2016), though triangle waves have also been adopted in position controlled tests to ensure a uniform test rate (Bennett and Kelly, 2013; Gardner-Morse and Stokes, 2004; Holsgrove et al., 2015a; Kotani et al., 2006). However, triangle waveforms may be less applicable in load control testing where the test rate will vary according to the stiffness of the specimen.

A key aspect of the comparisons of the present study was to transform the loads from the load cell datum to the geometric center of each specimen with a common orientation of coordinate system. This is an important step due to the different designs of GT1, GT2, and HEX, and the different locations of the load cell relative to the specimen. Previous studies investigating the stiffness matrices of single-level spinal specimens have used similar methods to transform load data to the center of the superior vertebral body (Holsgrove et al., 2015a; Stokes and Gardner-Morse, 2003), but many studies do not report if any transformation was completed, and this has the potential to greatly affect the results. For example, the use of a passive sub-assembly, such as that of GT2, is commonly adopted in pure moment testing of spinal specimens to minimize shear loading (Jaramillo et al., 2016; Kotani et al., 2006). However, the friction of a passive system, or the control limitations of an active system, may result in shear forces remaining, which could lead to substantial differences in the magnitude of moments at the specimen compared to the load cell datum. Likewise, the effect of the preload is likely to have a substantial effect, as the force of 500 N is sufficient to create considerable moments even when the lever arm of the load cell datum relative to the specimen center is small. Re-analysis of the GT2 tests of the present study without rigid body transformation confirms this, with a mean stiffness calculated at the load cell datum of 0.55–0.70 Nm/° less in flexion-extension and lateral bending with a 500 N preload compared to the stiffness at the center of the specimen.

The real-time load transformations on HEX were based around a fixed specimen center, which was defined once the specimen was mounted. The load transformations on GT1 accounted for the changes in the geometric specimen center based on axis translations during testing. Load transformations from GT2 did account for changes in the position of the specimen center in the z axis, but no changes in the x or y axes were accounted for, as no translational data was acquired from the passive XY platform. Based on GT1 data, the changes in the geometric center during testing were within 1 mm, and the stiffness based on a fixed specimen center differed by a maximum of only 0.03 Nm/° across all tests. Therefore differences in a fixed/mobile specimen center will not have affected the comparisons between the systems. However, changes in the specimen center may have a greater effect in tests using multi-segment specimens, or tests over large ranges of motion.

The stiffness and phase angle data from each system were used to calculate the 95% confidence intervals, which were used to produce upper and lower stiffness and phase angle limits (Table 3). It is recommended that the mean stiffness and phase angle should fall within the recommended limits in order to demonstrate test system equivalence. An increase in phase beyond the recommended limits may suggest system compliance, low clamp-to-clamp stiffness, or improper potting of the springs within the polymer. In such circumstances a high phase angle would often be accompanied by a reduction in the respective stiffness. It is additionally recommended that future studies report non-principal tracking error, in order to ensure that the target loading parameters are suitably met. The data of the present study suggest that shear loading can be adequately maintained within ±10 N using either the passive XY platform or active control, and non-principal moments can generally be maintained within ±0.5 Nm.

The present study builds upon previous recommendations to standardize in vitro spine testing (Goel et al., 2006; Holsgrove et al., 2015b; Wilke et al., 1998b) and demonstrates that by adopting a standardized pure moment testing protocol, the results of different multi-axis test systems can produce consistent stiffness measurements. However, the standardization must extend not only to the testing, but also to the rigid body transformation of loads, so that the stiffness is measured at a common position and orientation. This approach has led to recommended stiffness and phase angle limits measured at the center of standardized spring specimens. The testing protocol of the present study can be adopted by other research institutions to ensure equivalence of different multi-axis spine systems, which through the increased ability to compare in vitro tests, will benefit the spinal community as a whole.

Acknowledgements

This research was completed with the support of the Catherine Sharpe Foundation, the Enid Linder Foundation, and the University of Bath Alumni Fund.

Conflict of interest

The authors declare that they have no conflicts of interest.

References

Amin, D.B., Lawless, I.M., Sommerfeld, D., Stanley, R.M., Ding, B., Costi, J.J., 2015. Effect of potting technique on the measurement of six degree-of-freedom viscoelastic properties of human lumbar spine segments. J. Biomech. Eng. 137, 054501.

ASTM International, 2011. F2423–11 – Standard Guide for Functional, Kinematic, and Wear Assessment of Total Disc Prostheses. ASTM International, West Conshohocken, PA, USA.

Bennett, C.R., Kelly, B.P., 2013. Robotic application of a dynamic resultant force vector using real-time load-control: Simulation of an ideal follower load on Cadaveric L4–L5 segments. J. Biomech. 46, 2087–2092.

British Standards Institution, 2009. BS ISO 12189:2008 - Implants for surgery - Mechanical testing of implantable spinal devices - Fatigue test method for spinal implant assemblies using an anterior support. British Standards Institution, London, UK.

British Standards Institution, 2012. BS ISO 10243:2010+A1:2011 - Tools for pressing - Compression springs with rectangular section - Housing dimensions and colour coding. British Standards Institution, London, UK.

Chamoli, U., Korkusuz, M.H., Sabnis, A.B., Manolescu, A.R., Tsafnat, N., Diwan, A.D., 2015. Global and segmental kinematic changes following sequential resection of posterior osteoligamentous structures in the lumbar spine: An in vitro biomechanical investigation using pure moment testing protocols. Proc. Instit. Mech. Eng. Part H-J. Eng. Med. 229, 812–821.

Chung, S.M., Teoh, S.H., Tsai, K.T., Sin, K.K., 2002. Multi-axial spine biomechanical testing system with speckle displacement instrumentation. J. Biomech. Eng. 124, 471–477.

Costi, J.J., Hearn, T.C., Fazzalari, N.L., 2002. The effect of hydration on the stiffness of intervertebral discs in an ovine model. Clin. Biomech. 17, 446–455.

Costi, J.J., Stokes, I.A., Gardner-Morse, M.G., Iatridis, J.C., 2008. Frequency-dependent behavior of the intervertebral disc in response to each of six degree of freedom dynamic loading - Solid phase and fluid phase contributions. Spine 33, 1731–1738.

Cripton, P.A., Bruehlmann, S.B., Orr, T.E., Oxland, T.R., Nolte, L.P., 2000. In vitro axial preload application during spine flexibility testing: towards reduced apparatus-related artefacts. J. Biomech. 33, 1559–1568.

Ding, B., Cazzolato, B.S., Stanley, R.M., Grainger, S., Costi, J.J., 2014. Stiffness analysis and control of a stewart platform-based manipulator with decoupled sensor-actuator locations for ultrahigh accuracy positioning under large external loads. J. Dyn. Syst. Meas. Contr. 136. 061008-061008.

Ding, B.Y., Cazzolato, B.S., Grainger, S., Stanley, R.M., Costi, J.J., 2015. Active preload control of a redundantly actuated Stewart platform for backlash prevention. Robot. Comput.-Integrated Manuf. 32, 11–24.

Gardner-Morse, M.G., Stokes, I.A., 2003. Physiological axial compressive preloads increase motion segment stiffness, linearity and hysteresis in all six degrees of freedom for small displacements about the neutral posture. J. Orthop. Res. 21, 547–552.

Gardner-Morse, M.G., Stokes, I.A.F., 2004. Structural behavior of human lumbar spinal motion segments. J. Biomech. 37, 205–212.

Gay, R.E., Ilharreborde, B., Zhao, K., Boumediene, E., An, K.N., 2008. The effect of loading rate and degeneration on neutral region motion in human cadaveric lumbar motion segments. Clin. Biomech. 23, 1–7.

Goel, V.K., Panjabi, M.M., Patwardhan, A.G., Dooris, A.P., Serhan, H., 2006. Test protocols for evaluation of spinal implants. J. Bone Joint Surgery-American 88 (Suppl 2), 103–109.

Holsgrove, T.P., Gheduzzi, S., Gill, H.S., Miles, A.W., 2014. The development of a dynamic, six-axis spine simulator. Spine J. 14, 1308–1317.

Holsgrove, T.P., Gill, H.S., Miles, A.W., Gheduzzi, S., 2015a. The dynamic, six-axis stiffness matrix testing of porcine spinal specimens. Spine J. 15, 176–1884.

Holsgrove, T.P., Miles, A.W., Gheduzzi, S., 2017. The application of physiological loading using a dynamic, multi-axis spine simulator. Med. Eng. Phys. 41, 74–80.

Holsgrove, T.P., Nayak, N.R., Welch, W.C., Winkelstein, B.A., 2015b. Advanced multi-axis spine testing: clinical relevance and research recommendations. Int. J. Spine Surgery 9, 34.

Ilharreborde, B., Zhao, K., Boumediene, E., Gay, R., Berglund, L., An, K.N., 2010. A dynamic method for in vitro multisegment spine testing. Orthopaed. Traumatol.: Surgery Res. 96, 456–461.

Jaramillo, H.E., Puttlitz, C.M., McGilvray, K., Garcia, J.J., 2016. Characterization of the L4-L5-S1 motion segment using the stepwise reduction method. J. Biomech. 49, 1248–1254.

Jaumard, N.V., Welch, W.C., Winkelstein, B.A., 2011. Spinal Facet Joint Biomechanics and Mechanotransduction in Normal, Injury and Degenerative Conditions. J. Biomech. Eng. 133. 071010-071010.

Kelly, B.P., Bennett, C.R., 2013. Design and validation of a novel Cartesian biomechanical testing system with coordinated 6DOF real-time load control: application to the lumbar spine (L1–S, L4–L5). J. Biomech. 46, 1948–1954.

Kotani, Y., Cunningham, B.W., Abumi, K., Dmitriev, A.E., Hu, N.B., Ito, M., Shikinami, Y., McAfee, P.C., Minami, A., 2006. Multidirectional flexibility analysis of anterior and posterior lumbar artificial disc reconstruction: in vitro human cadaveric spine model. Eur. Spine J. 15, 1511–1520.

Lawless, I.M., Ding, B., Cazzolato, B.S., Costi, J.J., 2014. Adaptive velocity-based six degree of freedom load control for real-time unconstrained biomechanical testing. J. Biomech. 47, 3241–3247.

Martínez, H., Obst, T., Ulbrich, H., Burgkart, R., 2013. A novel application of direct force control to perform in-vitro biomechanical tests using robotic technology. J. Biomech. 46, 1379–1382.

Panjabi, M.M., Miura, T., Cripton, P.A., Wang, J.L., Nain, A.S., DuBois, C., 2001. Development of a system for in vitro neck muscle force replication in whole cervical spine experiments. Spine 26, 2214–2219.

Pflaster, D.S., Krag, M.H., Johnson, C.C., Haugh, L.D., Pope, M.H., 1997. Effect of test environment on intervertebral disc hydration. Spine 22, 133–139.

Stokes, I.A., Gardner-Morse, M., Churchill, D., Laible, J.P., 2002. Measurement of a spinal motion segment stiffness matrix. J. Biomech. 35, 517–521.

Stokes, I.A.F., Gardner-Morse, M., 2003. Spinal stiffness increases with axial load: another stabilizing consequence of muscle action. J. Electromyogr. Kinesiol. 13, 397–402.

Tawackoli, W., Marco, R., Liebschner, M.A., 2004. The effect of compressive axial preload on the flexibility of the thoracolumbar spine. Spine 29, 988–993.

Wheeler, D.J., Freeman, A.L., Ellingson, A.M., Nuckley, D.J., Buckley, J.M., Scheer, J.K., Crawford, N.R., Bechtold, J.E., 2011. Inter-laboratory variability in in vitro spinal segment flexibility testing. J. Biomech. 44, 2383–2387.

Wilke, H.J., Claes, L., Schmitt, H., Wolf, S., 1994. A universal spine tester for in vitro experiments with muscle force simulation. Eur. Spine J. 3, 91–97.

Wilke, H.J., Jungkunz, B., Wenger, K., Claes, L.E., 1998a. Spinal segment range of motion as a function of in vitro test conditions: effects of exposure period, accumulated cycles, angular-deformation rate, and moisture condition. Anatomical Record 251, 15–19.

Wilke, H.J., Kienle, A., Maile, S., Rasche, V., Berger-Roscher, N., 2016. A new dynamic six degrees of freedom disc-loading simulator allows to provoke disc damage and herniation. Eur. Spine J. 25, 1363–1372.

Wilke, H.J., Wenger, K., Claes, L., 1998b. Testing criteria for spinal implants: recommendations for the standardization of in vitro stability testing of spinal implants. Eur. Spine J. 7, 148–154.